

SEISMIC CHARACTERISTICS OF COMPLEX HALO-ANHYDRITES AND THEIR EFFECTS ON THE UNDERLYING CARBONATITES: A CASE STUDY OF THE RIGHT BANK OF THE AMU DARYA RIVER

TONGCUI GUO¹, HUAILONG CHEN², GUIHAI WANG³, HONGJUN WANG¹, MUWEI CHENG¹ and PENGYU CHEN¹

¹ PetroChina Research Institute of Petroleum Exploration and Development, Beijing 100083, P.R. China. guotc@petrochina.com.cn

² CNPC International (Turkmenistan), Ashgabat 744000, Turkmenistan.

³ PetroChina International Iraq FZE, Beijing 100034, P.R. China.

(Received April 26, 2016; revised version accepted May 29, 2017)

ABSTRACT

Guo, T.C., Chen, H.L., Wang, G.H., Wang, H.J., Cheng, M.W. and Chen, P.Y., 2017. Seismic characteristics of complex halo-anhydrites and their effects on the underlying carbonatites: a case study of the right bank of the Amu Darya River. *Journal of Seismic Exploration*, 26: 381-397.

Research on the impact of complex halo-anhydrites on seismic imaging of underlying carbonates has been a focus of seismic exploration. Here, this research analyzed for the first time the seismic reflection characteristics of sandwich-structured halo-anhydrites on the right bank of the Amu Darya, having three anhydrite layers and two halite layers. The reflections from the upper halite displayed a set of weak amplitude reflection and gentle seismic events. Reflections from middle anhydrite, lower halite, and lower anhydrite showed intense reflected energy and distorted events with poor continuity. Three theoretical models, an "eyeball" salt dome model, thick salt model, and two-layer thin salt model, and two actual complex halo-anhydrite models were designed. Seismic forward modeling and illumination analysis were performed on the theoretical and empirical models using a staggered-grid high-order finite-difference method on an acoustic equation in an inhomogeneous medium. The results indicated several important points. First, interference waves generated by the halo-anhydrites, such as the strong energy multiples, wide-angle guided waves, scattered waves, and bow-ties, reduced the SNR (signal-to-noise ratio) and continuity of reflections from underlying strata. Second, bow-ties formed by complex halo-anhydrites causing false bright spots on the reflection amplitude from the underlying strata. Third, the number of halo-anhydrite layers had a more remarkable shielding effect on energy from underlying strata than thickness. Finally, the complex structure of halo-anhydrites led to heterogeneity in the downward propagating seismic energy and formed illumination shadows. In the study area, deformed halo-anhydrites demonstrated seismic characteristics like "eye-ball shaped halite" and "anhydrite caps". The effects of thickness and level of deformation of these halo-anhydrites on the formation of gas reservoirs in the underlying carbonate, the height of the gas column, and the structure of the top of the gas reservoir, are noteworthy. Lateral sealing of the strongly deformed halo-anhydrites play a key role in the underlying patch reef gas reservoir. Underlying anhydrites near the gas-water interface are beneficial for improving the porosity of the porous carbonate reservoir.

KEY WORDS: halo-anhydrites, seismic facies, seismic reflection features, seismic wave illumination, acoustic simulation.

INTRODUCTION

The Amu Darya basin is a large salt basin in central Asia rich in natural gas. The main body is situated in eastern Turkmenistan and southwestern Uzbekistan. The right bank of the Amu Darya lies within the country of Turkmenistan. It is located on the Amu Darya northern fault, across three second-order structural units from west to east, and trending NW-SE. The elevation is higher in the east, west and north, and lower in the middle and south, Fig. 1 shows the regional structural map of the Amu darya right bank area.

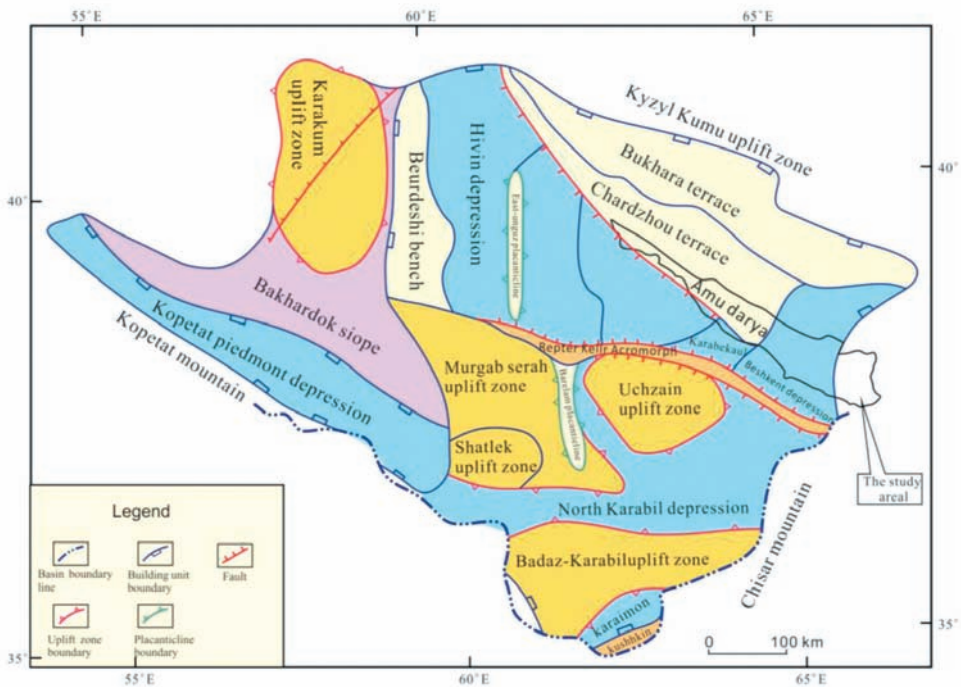


Fig. 1. the regional structural map of the Amu darya right bank area.

On the right bank of the Amu Darya, the well-developed upper Jurassic halo-anhydrite deposits cover the entire region. The sediment profile is divided into five alternating layers from bottom to top: lower anhydrite, lower halite, mid anhydrites, upper halite and upper anhydrite, forming a sandwiched structure with a thickness of 100 ~ 1800 m. The structure is thinner on the west and thicker on the east, forming an east-west zoning. Vertically it presents

multiple cycles and rhythms with strong deformation and complex structure within layers, and a large variation in thickness. The ground surface shows unevenness. Due to energy shielding and interference caused by the halo-anhydrites, the sub-salt target carbonates show serious distortion in the reflected signal, discontinuity in events and poor image quality in time-domain seismic profiles, which result in difficulty consolidating the carbonate structure and predicting reservoirs (Lv and Liu, 2013).

Based on analysis of seismic reflection characteristics of halo-anhydrites in the study area and a staggered-grid high-order finite-difference method on an acoustic equation in inhomogeneous medium this study performed forward modeling and illumination analysis on theoretical and actual models of complex deformed halo-anhydrite structures. The impact of seismic wavefield characteristics, waveforms and propagation, and the presence of a complex salt dome on the sub-salt reflected wavefield were analyzed based on the forward modeling. Based on seismic illumination analysis, the seismic wavefield energy characteristics of the halo-anhydrites and the shielding effect on the sub-layer waves are discussed. Furthermore, the influence of complex halo-anhydrites on seismic imaging of the sub-layer carbonates was analyzed, which could be significant for the structural confirmation of carbonates, reef identification and improving seismic exploration in the region.

SEISMIC REFLECTION CHARACTERISTICS OF HALO-ANHYDRITES

The seismic reflection structure of the halo-anhydrites at the right bank of the Amu Darya is divided into two parts. The upper part is composed of upper anhydrite and upper halite, and the lower part is composed of middle anhydrite, lower halite and lower anhydrite. The structural deformation of the upper part is weak, and deformation of the lower part is strong.

The seismic reflection characteristics of the upper halo-anhydrites are as follows. First, seismic reflection events from the top surface of the upper anhydrite occur between the Lower Cretaceous clastic and Upper Jurassic halo-anhydrites, and show a distinct lithologic interface, corresponding to wave peaks with strong reflection amplitude, good continuity and stable horizontal features, and are easy to track. The thickness of the upper anhydrite is 7-15 m. Second, the upper salt shows a weak-amplitude reflection characterized by blank to discontinuous middle and low frequency weak parallel reflection events. When mud strips or anhydrite layers are present locally, parallel reflection events are observed. The thickness of the upper salt is 50-800 m, with gradual thickening from west to east.

According to the seismic reflection of the lower halo-anhydrites and degree of deformation of lower halite and anhydrite, the halo-anhydrite profile

is divided into three types from west to east: no deformation, containing strong crumpled deformation and containing rheological features. Much of the central and eastern region of right bank develop halo-anhydrites with strong crumpled deformation, with undeformed halites only found in the western region, which is characterized by a series of parallel reflection waves with strong continuity. Fig. 2 shows the seismic and geological profiles with the undeformed halo-anhydrites. The seismic reflection of halo-anhydrites with rheological features is characterized by discontinuous intense dense reflected waves. The lower halite is thin, and the middle and lower anhydrites are fragmented. Fig. 3 shows the seismic and geological profiles with the rheological halo-anhydrites. This paper mainly describes the seismic reflection characteristics of strongly crumpled and deformed halo-anhydrites. Fig. 4 shows the seismic and geological profiles with the deformed halo-anhydrites.

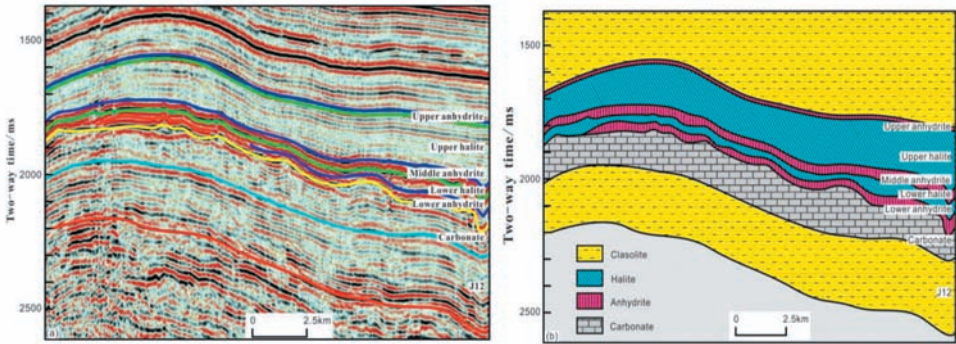


Fig. 2. Seismic profile with undeformed halo-anhydrites (a) and geological profile (b).

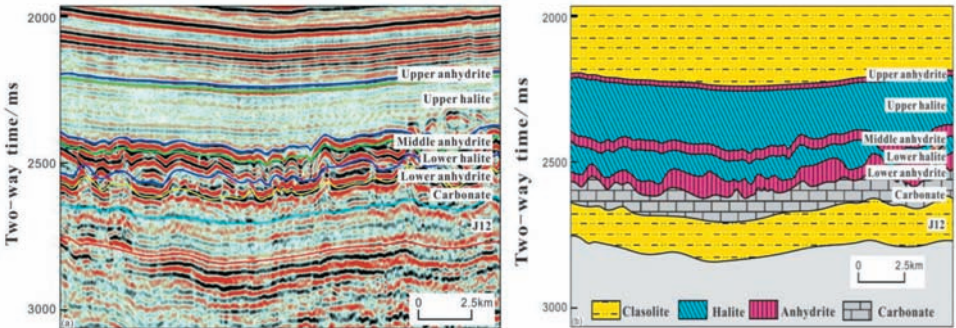


Fig. 3. Seismic profile with rheological halo-anhydrites (a) and geological profile (b).

Seismic reflection characteristics of halo-anhydrites with severely crumpled deformation were as follows. (1) Intense reflections from middle anhydrite correspond to wave peaks. The reflection energy is high, but due to plastic deformation of lower halite, crumpling and deformation are severe. (2) The lower halite shows reflection waves with typical "eyeball" characteristics, with weak-amplitude blank reflection at the center of "eyeball" and strong-amplitude, low-frequency and relatively continuous reflection in the middle of upper and lower "eyelids". Uneven amplitude and disordered events are observed at the sides of lower "eyelid". (3) The lower anhydrite is located at the thickened part of the "bridge" between the two "eyeballs", forming a cap on the underlying carbonate reef. Both the cap and the underlying reef patches show random reflections. (4) The interface between lower halite and anhydrite is difficult to trace continuously. Relatively continuous and strong reflections are observed at positions underlying the "eyeball", but the interface became difficult to identify at positions between the "eyeballs". Seismic reflections there show strong fluctuations in strength with poor continuity. The underlying reefs also caused intense local crumpling.

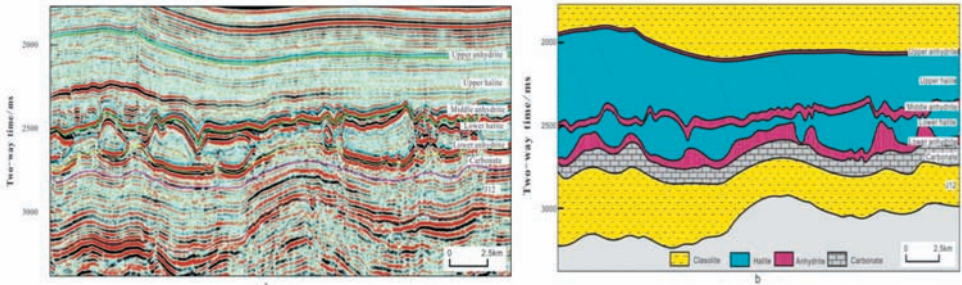


Fig. 4 Seismic profile with severely crumpled and deformed halo-anhydrites (a) and geological profile (b).

FORWARD MODELING OF HALO-ANHYDRITE SEISMIC RESPONSE

Based on theoretical and empirical models of complex halo-anhydrites, this paper focuses on the influence of the severely crumpled and deformed halo-anhydrites on the seismic response of the sub-salt carbonates.

Theoretical modeling

An "eyeball" salt dome model was designed to mimic the "three anhydrites, two halites" geological structure of the Amu Darya right bank and

its typical "eyeball" seismic facies characteristics (Fig. 5). Through forward simulation on the theoretical model, the seismic wavefield characteristics, pattern of seismic wave propagation and influence of the salt dome on the underlying reflected wavefield were analyzed. The theoretical model was 6 km * 2 km in size, with 5 m * 5 m grid size for numerical simulation, and 0.5 ms sampling interval. The explosion source was located at (3 km, 0), with dominant wavelet frequency of 30 Hz. Full wavefield forward modeling was carried out using the inhomogeneous medium acoustic wave equation (Mou and Pei, 2004).

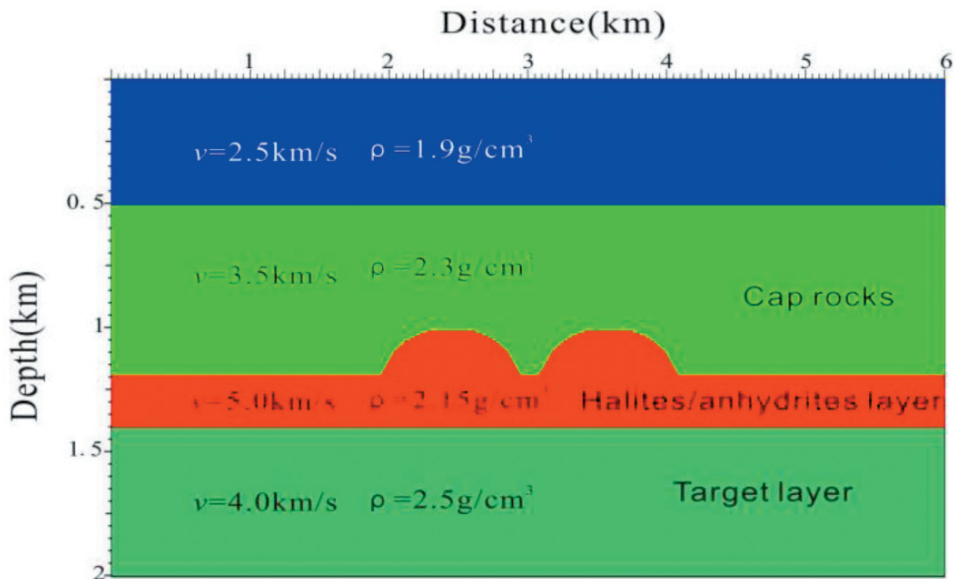


Fig. 5. Geological model of the "eyeball" salt dome.

Fig. 6 is a single-shot record and wavefield snapshot of the "eyeball" salt dome model simulated using the acoustic wave equation. The explosion source for Fig. 6a was located between the two salt domes at (3 km, 0), and in Fig. 6b above the left salt dome at (2.5 km, 0). Several observations are made based on Fig. 6. (1) Dome-shaped halo-anhydrites caused distinguishable energy focusing in the reflected and scattered wavefield, with strong modulating effect on the wavefront of transmitted and reflected waves. High-energy high-speed guided waves produced strong interference within the halo-anhydrites. (2) Interference such as multiple scattered waves, bow-ties, and multiples from the dome-shaped halo-anhydrites affected the reflected signal from underlying strata, reducing the signal-to-noise ratio. (3) Reflection from top of the dome had clear features, but the irregular shape and large variation in salt dome thickness caused non-uniformity in the reflected energy of underlying strata. The irregular shape

seriously altered the propagation path of seismic waves, producing a variety of diffraction and scattering, and forming strong superimposed interference waves that interfered with the signal. These showed up in the profile as energy fluctuations with random and disordered waveform, and caused focusing of high-energy, high-speed guided waves at irregular turning points around the salt dome. Between the two salt domes, seismic waves with inhomogeneous energy were formed at the top of sub-salt target layer, in agreement with the seismic reflection characteristics of the seismic profile of the Amu Darya right bank. Random, non-uniform reflections between the "salt eyeballs" occurred at the location of reef growth in the sub-salt target layer. This location has thin lower halite and thick lower anhydrite, with the seismic profile showing cluttered seismic facies. The irregular shape and uneven thickness of halo-anhydrites augmented the disordered seismic reflection and uneven reflected energy of the sub-salt reef top.

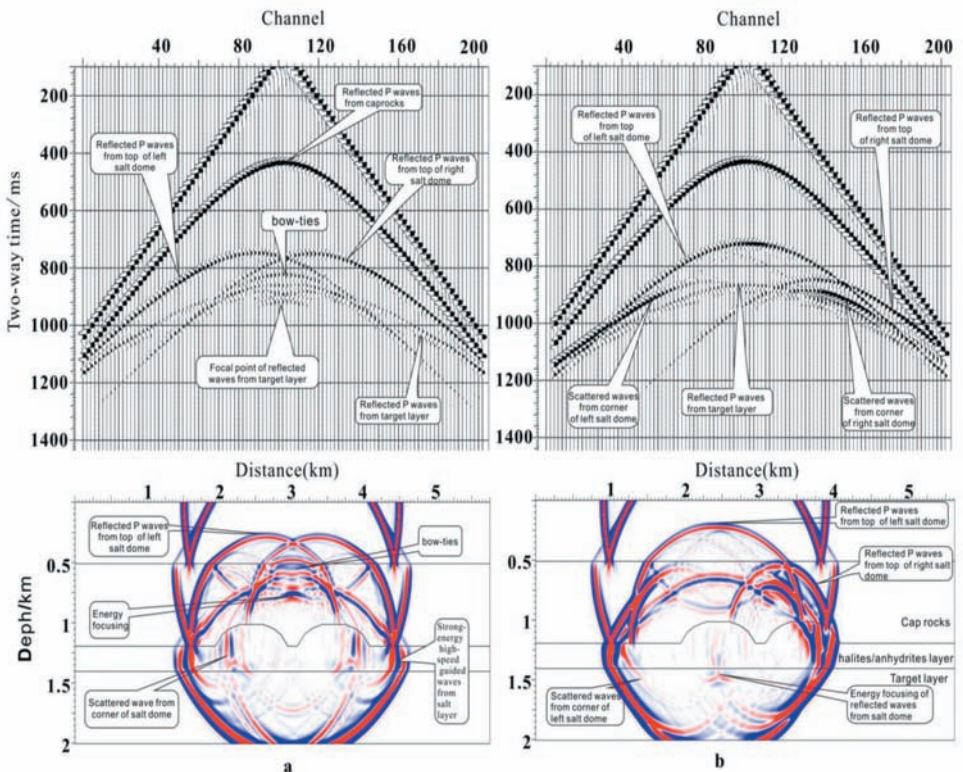


Fig. 6. Record of single-shot acoustic simulation of the "eyeball" salt dome (upper) and wavefield snapshot (lower) ($t = 600$ ms) source a located mid-way between the two salt domes (3 km,0); source b located above the left dome (2.5 km,0).

Actual model for complex halo-anhydrite formation

Fig. 7 shows the actual velocity model for the complex halo-anhydrite structure, with 36 km * 4 km model size and 10 m * 5 m grid. The model was constructed with seismic horizons as constraints, by interpolation and extrapolation of acoustic velocity curves of the seven wells after well-to-seismic calibration. The velocities of the surface layers was 2.0 km/s. The forward simulation was carried out using a staggered-grid high-order finite-difference method. The simulation parameters were: double shot with 100 m spacing and 360 shots total. The dominant wavelet frequency of the explosion source was 30 Hz. Each shot was received with 200 channels placed 25 m apart. Fig. 8 shows the single-shot acoustic simulation on actual complex halo-anhydrite model with explosion source at (15 km, 0), and Fig. 9 is the acoustic simulation profile of actual model with zero offset. In the single-shot record and zero offset profile, the four layers of halo-anhydrites between the upper and lower anhydrites showed distinct characteristics in reflected waves, especially the appearance of energy focusing at the depression turning point in the lower salt dome (circled by an ellipse in the figure). This non-uniform halo-anhydrite layer produces strong distortion and scattering, and energy shielding of the seismic wavefield, resulting in weak wave transmission and inconsistency in the reflected signal from sub-salt target layer, as well as an uneven variation in signal amplitude and poor continuity.

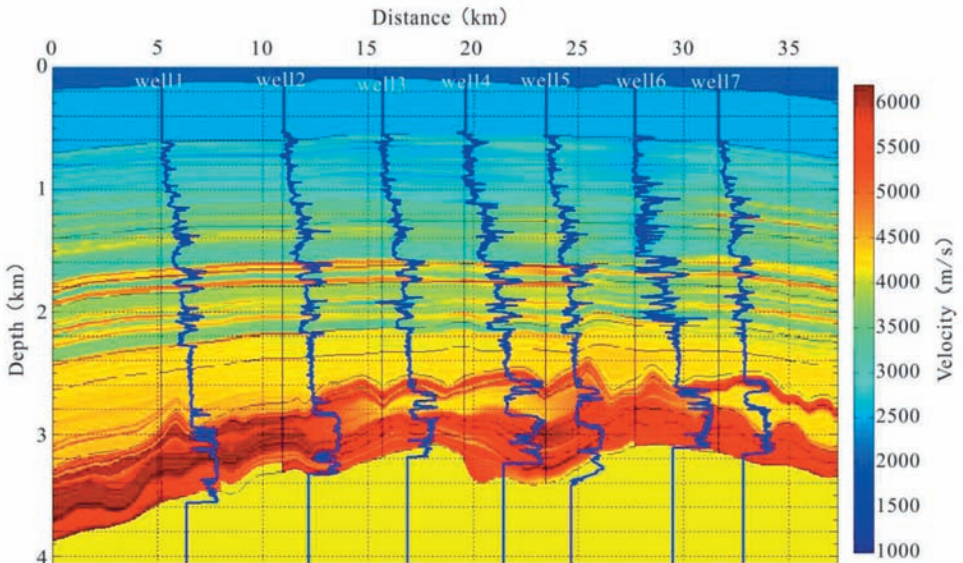


Fig. 7. Velocity model of actually complex halo-anhydrites.

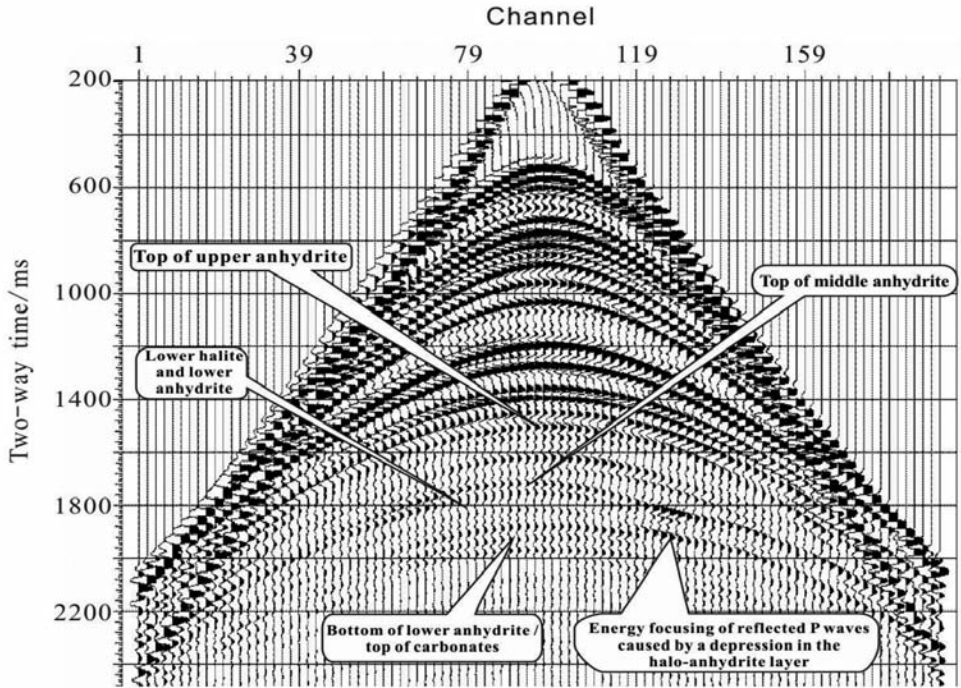


Fig. 8. Record of single-shot acoustic simulation on actual halo-anhydrite model [explosion source at (15 km,0)].

Figs. 9a and 9b show the actual seismic pre-stack time migration profile and forward modeling pre-stack time migration profile. Both figures share identical main features, with differences in detail. In the cross-section of the complex halo-anhydrite actual model in Fig. 7, a large-scale lower salt dome at the position of well #5 is shown. Drilling revealed a thickness of 258 m for lower halite, and 203 m for lower anhydrite, with the top of underlying carbonates at a depth of -3244 m. At the position of well #2, the lower halite was very thin, only 9 m, and the lower anhydrite was 302 m thick, with the top of carbonates at -3261 m. For the two wells, there was only a 17 m difference in the depth to the top of carbonates. In Fig. 10a, the actual time domain seismic profile shows that the top of carbonates in well #5 (yellow layer circled by ellipse in Fig. 10a) was obviously lower in seismic reflection time, by almost 100 ms, compared with well #2, a false disagreement between the time profile and depth profile. From the forward modeling pre-stack time migration profile shown in Fig. 10b, the reflection times of top of the carbonates for well #5 and #2 were close, as seismic reflection time simulated using an accurate velocity

model should agree with depth in the geological model. Inconsistency would otherwise exist between time and depth profiles due to unevenness in the complex halo-anhydrite layer thicknesses and velocities. Pre-stack depth migration should be applied to the imaging of strata with complex halo-anhydrite layers on top, so that false depth changes do not occur.

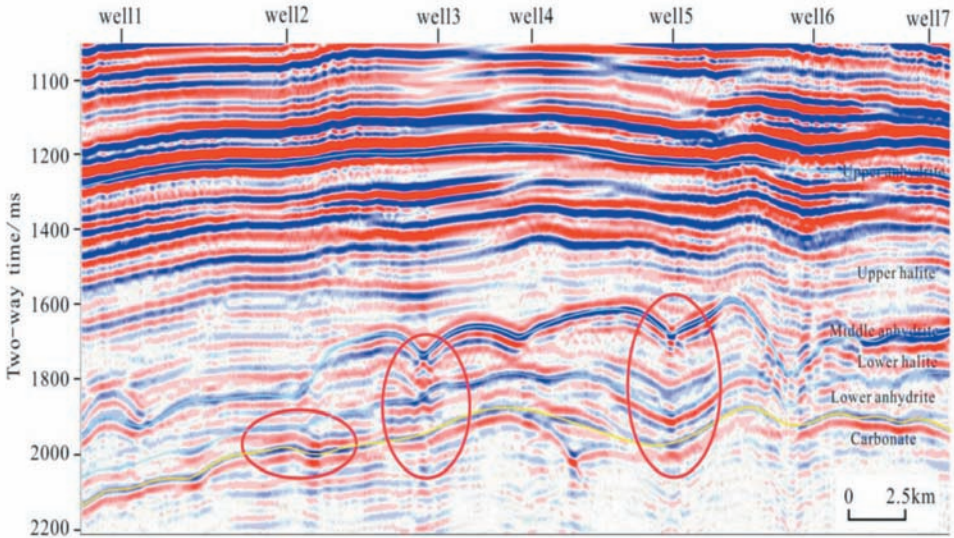


Fig. 9. Cross-section of zero offset acoustic simulation on an actual halo-anhydrite model.

CHARACTERISTICS OF SEISMIC WAVE ENERGY PROPAGATION IN HALO-ANHYDRITES

In the study area, the halo-anhydrites show multiple cycles and multiple rhythms in the vertical direction. To study the effect of halo-anhydrite layers, and their thicknesses, on energy shielding of seismic waves, this research designed theoretical and empirical models with different layers and thicknesses. Fig. 11a shows a layered geological model with 400 m thick halite (or anhydrite). Fig. 11b illustrates a model containing two thin halite (or anhydrite) layers of 50 m and 200 m thickness, whereas Fig. 11c is the "three anhydrites, two halites" structure model. The energy distribution and propagation of seismic waves in different structures of halo-anhydrites were analyzed using the seismic wave equation illumination on the three models.

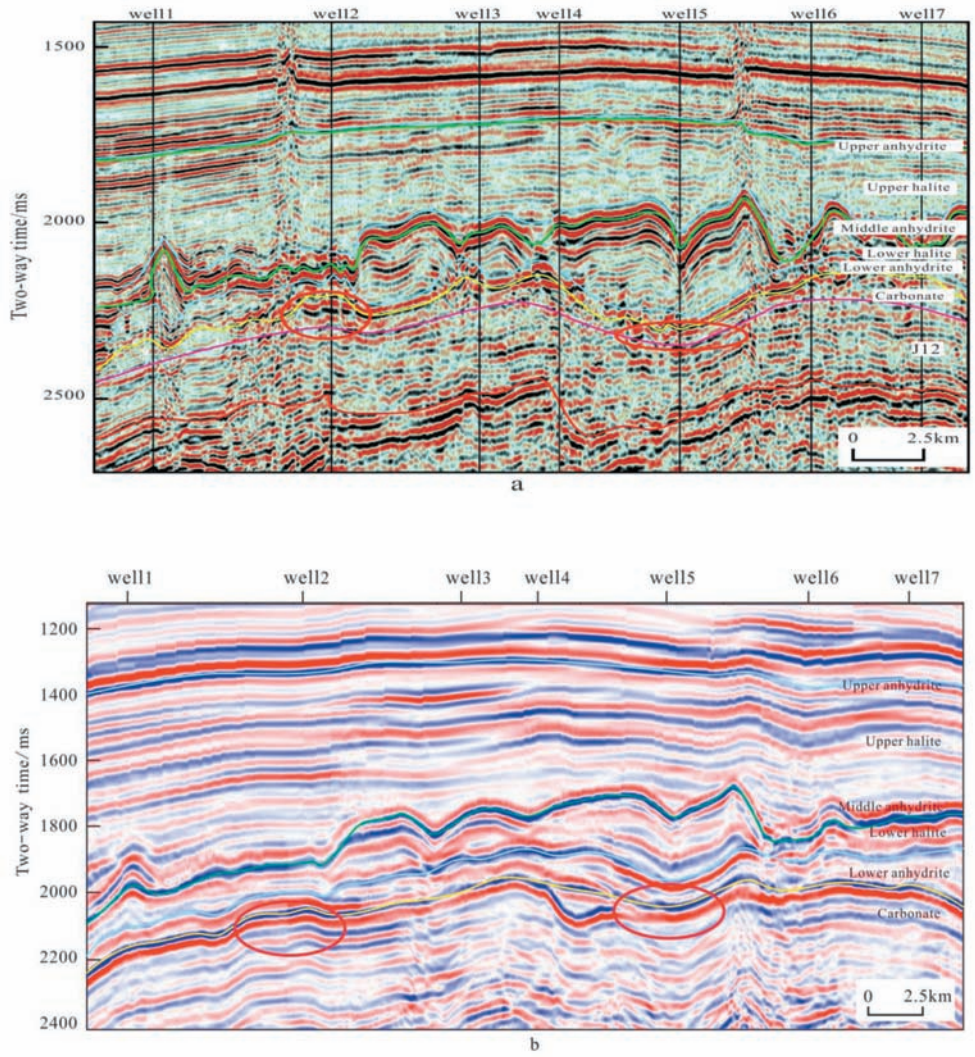


Fig. 10. Cross-section of actual halo-anhydrite model pre-stack time migration (a) and cross-section of forward simulation pre-stack time migration (enhanced) (b).

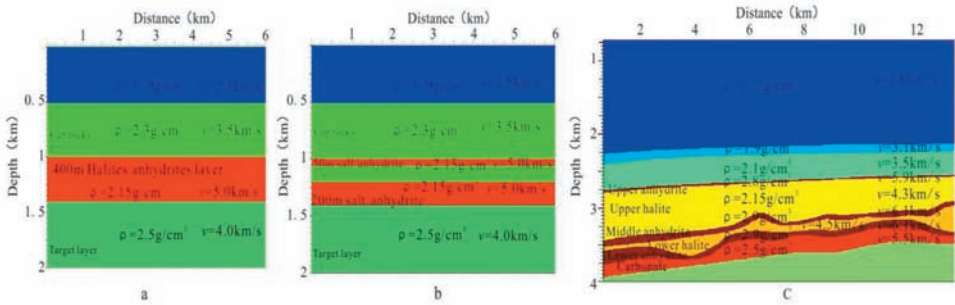


Fig. 11. Geological models for thick halite (or anhydrite) layer (a), two thin layers of halite (or anhydrite) (b) and complex halo-anhydrite layers (c).

Fig. 12 shows the single-shot acoustic illumination images of halo-anhydrites with different thicknesses and layers. Through seismic illumination analysis, the following conclusions can be drawn. (1) As the thickness of halo-anhydrite layers increased, the energy shielding effect on sub-salt layers was enhanced. (2) As the number of halo-anhydrite layers increased, the energy shielding effect on sub-salt layers was enhanced. The influence of layer number was greater than thickness.

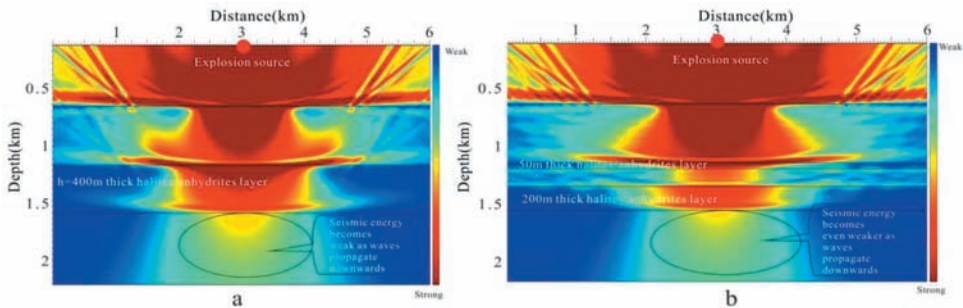


Fig. 12. Full wavefield single-shot acoustic illumination for 400 m thick halite/anhydrite layer (a) and double halite/anhydrite layers (b)

Fig. 13 shows the single-shot acoustic illumination image of complex halo-anhydrite model with the shot location at (5 km,0). Energy was transmitted unevenly through the upper anhydrite and halite layers. In the middle anhydrite layer, with high transmission speed, illumination showed a dark red color and energy was concentrated. Energy reaching the lower halite through the middle anhydrite was not uniform. In the lower anhydrite, energy appeared even more

inhomogeneous. Still less energy made its way through the lower anhydrite, showing weaker and non-uniform illumination. This indicates that the three irregularly structured anhydrite layers provided more energy shielding than the halite layers, and energy concentrated within these layers, providing shielding for the underlying target carbonate layer. The complex halo-anhydrite structure caused non-uniform downward seismic energy propagation, such that inconsistency in energy stacking occurred in the target layer below, further affecting the image quality and seismic interpretation of the sub-layers. The boundary shape of the salt (or anhydrite) dome had more influence on imaging than the top of the dome did, which can be reduced by illumination compensation on migration imaging.

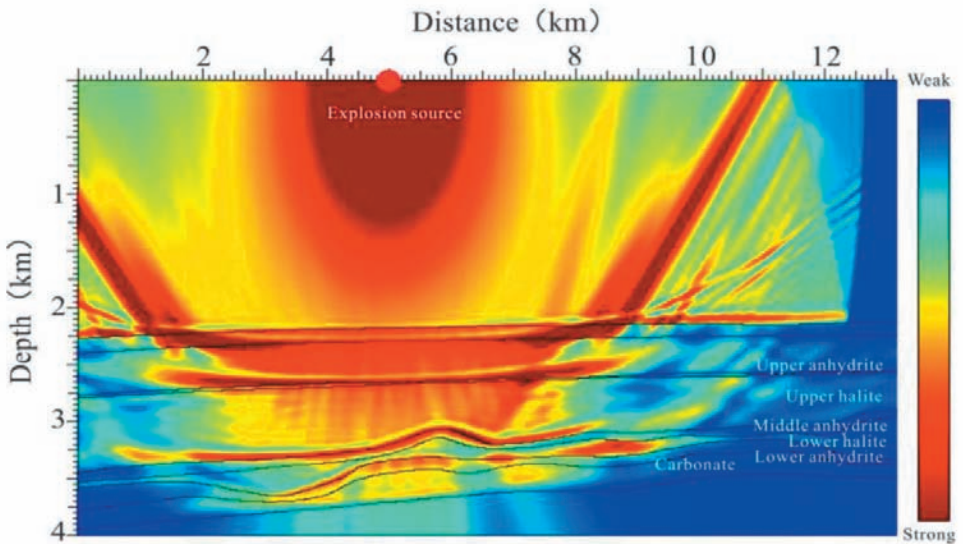


Fig. 13. Full wavefield single-shot acoustic illumination for the "three anhydrites, two halites" formation model [explosion position at (5 km, 0)].

Controlling effects of halo-anhydrites on the underlying carbonatite reef distribution

In areas where halo-anhydrites are strongly crushed and distorted, the underlying carbonatites consist mainly of reef gas reservoirs. The developmental thickness of the reefs is intimately associated with the thickness and the degree of deformation in the halo-anhydrites. In the patch reef development area, these associations are often characterized by the intense deformation on both sides of the reef, uplifting of the center reefs, eye-shaped lower halite layers on the sides, and mirror symmetry in the thickness of the lower halo-anhydrite layers

and the carbonatite layer. This characteristic is an important marker differentiating the patch reefs in the right bank of the Amu Darya River. In the strongly deformed halo-anhydrites, the size, gas column height, and gas-water interface of the underlying carbonatite gas reservoir depend on the size of the lower halite domes. Lateral sealing of the lower halite domes is critical for the formation of gas reservoir in the patch reefs. Fig. 14 shows the seismic profiles of the lower halite domes and the patch reef gas reservoirs in the slope, located in the middle of the right bank of the Amu Darya river. In this figure, a lithological trap was formed in the upward direction from the sealing of a thrust fault and a salt dome on the hanging wall (yellow layer circled by ellipse in Fig. 14). Previous drillings have showed that the reefs in the slope are close to a petroleum source, which provides preferential access to oil and gas. As long as the conditions favor the lateral sealing of the lower halite dome, gas reservoirs will be formed. Fig. 15 presents the overlay of the lateral sealing of halite domes and reef distribution in the area where halo-anhydrites are strongly deformed. This figure shows that reef gas reservoirs are well-formed in areas where lateral halite dome shelters are found. In the figure, the colored polygons represent the reef boundaries, while the dark blue polygons represent the boundaries laterally sealed by the lower halite domes.

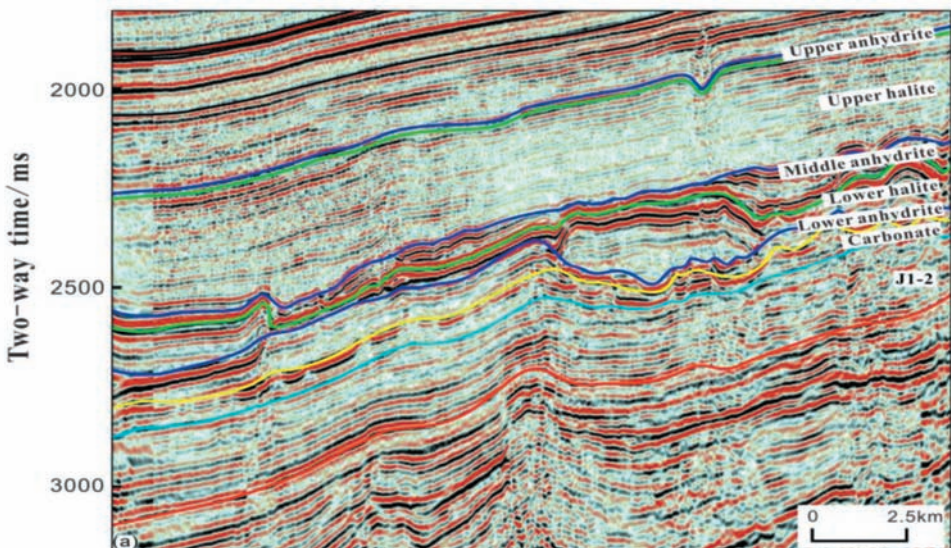


Fig. 14. Seismic profiles of the reef reservoirs and halite domes.

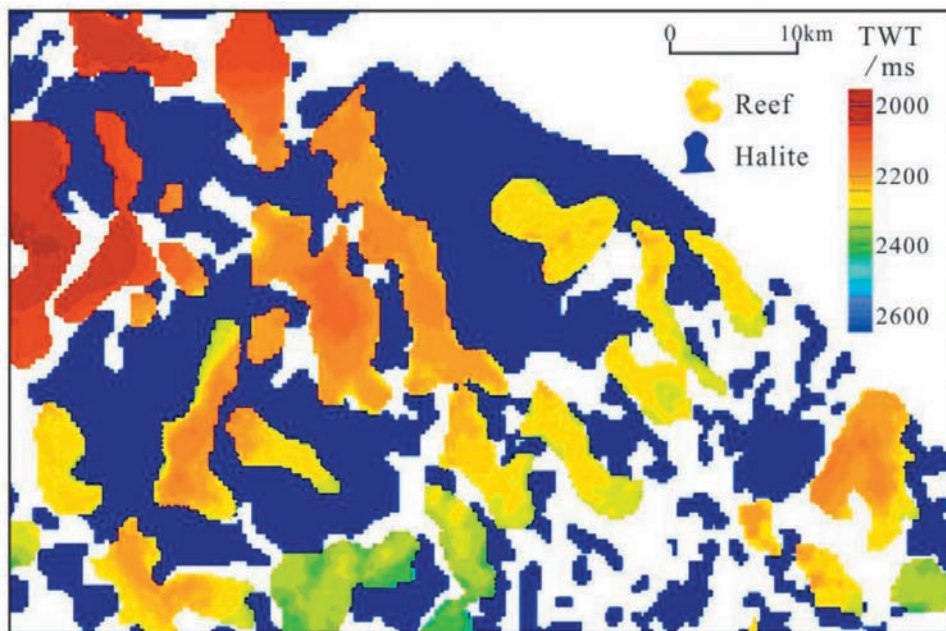


Fig. 15. Overlay of the reefs and lower halite domes in the study area.

Effects of anhydrites on the corrosion of underlying porous carbonatite reservoirs

Carbonatite gas reservoirs in the middle and eastern part of the right bank of the Amu Darya River are rich in H_2S . Studies have found that on the side of the uplifted trust fault with a broken fold belt, if the lower anhydrite layer and porous carbonates are connected, the lower anhydrite layers are dissolved around the gas-water interface of the porosity-developed carbonatite reservoirs. In these anhydrite layers, sulfate ions tend to react with heavy hydrocarbons in a H_2S -generating reaction, termed the "thermochemical sulfate reduction" (TSR). Corrosion caused by the H_2S increases the porosity of the porous carbonatite reservoirs, thereby improving the reservoir layers of carbonatite reservoirs. Fig. 16 shows the location patterns of the zones corroded by anhydrites in the porous carbonatite reservoirs.

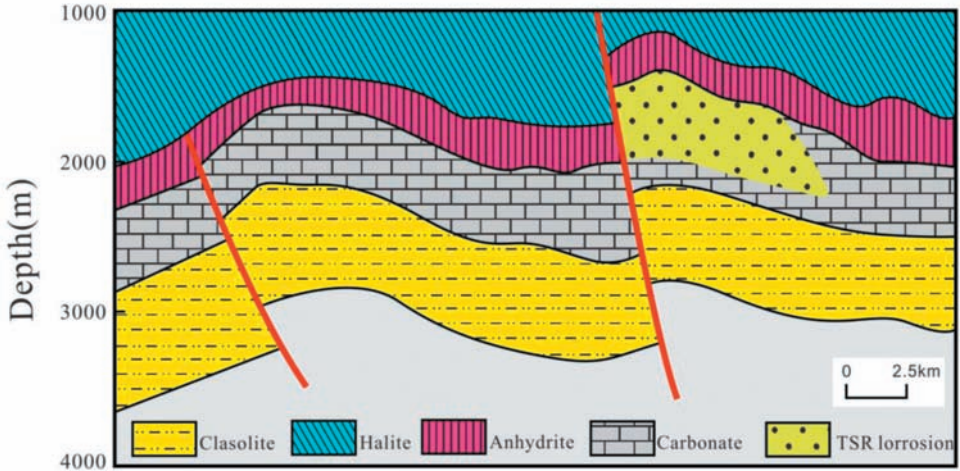


Fig. 16. Location patterns of anhydrite-corroded zones in the porous carbonatite reservoir.

CONCLUSIONS

The complex halo-anhydrites with a "three anhydrites, two halites" structure at the Amu Darya right bank showed the following features in seismic cross-section. The upper anhydrite and halite reflection events showed gentle variations, with strong reflection amplitude and good continuity from the upper anhydrite. The upper halite showed a group of blank and weak-amplitude reflected waves. Seismic events were severely distorted for the middle anhydrite, lower halite and lower anhydrite, as denoted by strong energy waves. At the irregular boundaries of the lower "eyeball" and lower "anhydrite cap", seismic reflection waves were disordered and had poor continuity.

High-energy multiple waves, wide-angle guided waves, scattered waves and bow-ties are more likely to be generated in a complex halo-anhydrite structure. These waves interfere with the reflected signal from the underlying carbonates, particularly at the turning points of the salt dome, where energy focusing of high-speed guided waves occurs and reduces the signal-to-noise ratio.

As halo-anhydrite layer thickness increases, the shielding effect on the energy from sub-salt layers also increases. As the number of halo-anhydrite layers increases, shielding increases. The effect of layer number is greater than the effect of thickness.

The boundary shape of the halite (or anhydrite) dome has an even more pronounced impact on the imaging of underlying layers than the top of the salt dome. Halo-anhydrite layers with irregular thickness and structure cause a high degree of distortion and scattering, as well as energy shielding in the seismic wavefield. This results in a non-uniform downward propagation of transmitted energy, which significantly impacts the imaging quality of the underlying carbonates and description of reefs.

The thicknesses of the strongly deformed halo-anhydrites and the underlying patch reef show mirror symmetry.

The lateral sealing of the halo-anhydrites plays an important role in the formation of the underlying patch reef gas reservoirs and in determining the height of the gas column. When the lower halite domes and the porous carbonatite reservoir are connected, chemical reactions are easily triggered near the gas-water interface, which help improve the porosity of the carbonatite reservoir.

REFERENCES

- Lv, G.X. and Liu, H.N., 2013. Sub-salt carbonate large gas field exploration and development in the right bank of the Amu Darya. Science Press, Beijing: 50-52.
- Mou, Y.G. and Pei, Z.L., 2004. Seismic numerical modeling for 3-D complex media. Petroleum Industry Press, Beijing: 45-59.